Study of the high-efficiency fuelling features of supersonic molecular beam injection on HL-2A tokamak

D. L. Yu[a)], C. Y. Chen[a)], L. H. Yao[a)], J. Q. Dong[a,b)], B. B. Feng[a)], Y. Zhou[a)], Z. B. Shi[a)], J. Zhou[a)], X. Y. Han[a)], W. L. Zhong[a)], C. H. Cui[a)], Y. Huang[a)], Z. Cao[a)], Yi Liu[a)], L. W. Yan[a)], Q. W. Yang[a)], X. R. Duan[a)] and Yong Liu[a)]

a) Southwestern Institute of Physics, Chengdu, China

b) Institute for Fusion Theory and Simulation, Zhejiang University, Hangzhou, China

1. Introduction

High fuelling efficiency, simple structure, and good flexibility make the supersonic molecular beam injection (SMBI) popular; and the SMBI is utilized both on tokamaks and stellarators. On HL-2A, the penetration of SMBI is studied by D_α arrays (a CCD camera is available alternatively) and the fuelling efficiency is evaluated[1]. The fuelling efficiency of SMBI is around 30~60% for Ohmic heated and limiter plasma. In order to study the high fuelling efficiency features of SMBI, comparisons of the GP and SMBI are carried out on HL-2A[2]. Normalized by fuelled particle inventory, the D_α emission induced by SMBI is about 50% higher than that of GP, indicating that higher percentage of fuel injected by SMBI will enter the plasma. Strong particle convection (inward pinch) is observed with hydrogen cyanide (HCN) interferometer as the densities from the core and edge channels increase and decrease, respectively, in the post-fuelling phase. In addition, microwave reflectometry (MWR) indicates that the peak of fuelled density moves inward. By comparing the SMBI pulses with and without electron cyclotron resonance heating (ECRH), it is identified that the pinch is driven by the enhancement of electron temperature gradient. It is observed that higher enhancement (up to twice) of normalized electron temperature gradient for SMBI than that for

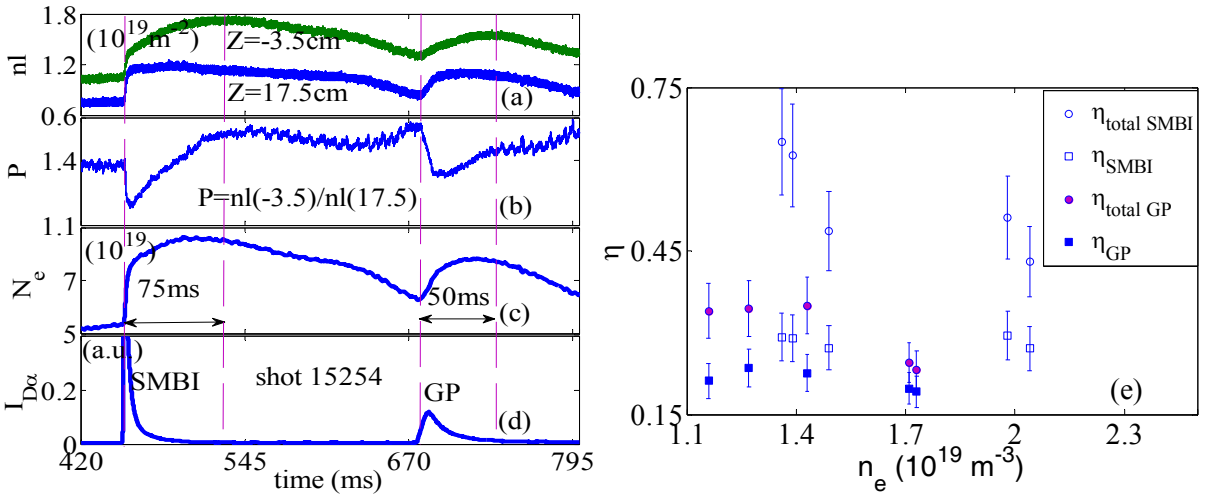

Figure 1. Comparison of fuelling efficiency between GP and SMBI. Line-integrated density (a); the peaking factor (b); the electron numbers (c); D_α monitoring the fuelling (d); the fuelling efficiency of GP and SMBI (e).

GP, and this is another mechanism for higher fuelling efficiency of SMBI.

2. Experimental results

2.1 Comparison of fuelling efficiency between GP and SMBI

Conventionally, the definition of the fuelling efficiency is comparing the growth rate of total particles (dN_e/dt) before and after the termination of GP (SMBI) with fuel flow rate of Φ_f,

$$\eta = \frac{(dN_e/dt)_{before} - (dN_e/dt)_{after}}{\Phi_f} \qquad (1)$$

By neglecting the $(dN_e/dt)_{after}$ in equation (1), the fuelling efficiency (η) can be rewritten as the ratio of time derivative of particle increment and fuelling influx, i.e. $\eta = N_e'/\Phi_f$; as the plasma inventory continues to increase after the fuelling pulse, another fuelling efficiency (η_{total}) is defined as the ratio of maximum increment of electron numbers (ΔN_e) and the injected inventory (N_{Fuel}), i.e. $\eta_{total} = \Delta N_e/N_{Fuel}$. In shot 15254, a 12-millisecond GP (3.1×10^{19} D_2) and a 1-millisecond SMBI (2.4×10^{19} D_2) are performed, as shown in figures 1(a), (b) (c) and (d). The peaking factor reaches the maximum at about 75 ms after the SMBI pulse and much higher than pre-SMBI; in the case of GP, the peaking factor recovers 50 ms after the GP pulse but not as high as pre-GP phase, as shown in figure 1(b). Besides, five contrast discharges (15251~15255) are performed. The results indicate that the fuelling efficiency η is about 0.19~0.24 and 0.27~0.30 for GP and SMBI, respectively; while η_{total} is about 0.23~0.34 and 0.43~0.65 for GP and SMBI, respectively, as shown in figure 1(e). Both η and η_{total} of SMBI are obviously higher than those of GP. The total fuelling efficiency (η_{total}) of SMBI is approximately twice as high as that of GP.

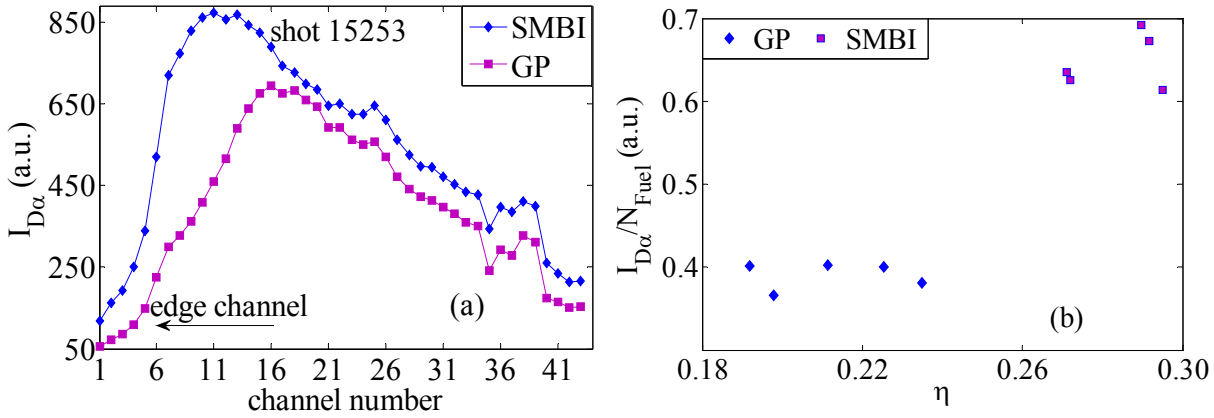

Figure 2. Chord profiles of D_α (a) and normalized D_α intensity for GP and SMBI (b)

$I_{D\alpha}$ and N_{Fuel} represent the D_α intensity and fuelled particle inventory, respectively.

2.2 Comparison of normalized D_α emission between GP and SMBI

The time integrated D_α emission represents the influx of the neutral deuterium particles. The D_α emission normalized by the injected inventory is utilized to investigate the effective fuel entering the plasma edge, as shown in figure 2. Figure 2(a) shows the chord D_α emission from the tangential array. The D_α emission induced by SMBI is much peaked than that of GP. However, the intensity decreasing trend along the channel number indicates that the D_α spot of SMBI is not smaller than that of GP, as the distance of SMBI nozzle is 1.28 m away from the plasma edge whereas the distance is about 0.1 m for the GP. The normalized D_α intensities of SMBI and GP are about 0.65 and 0.39, respectively, indicating that higher percentage of the neutrals injected by SMBI enter the plasma than that by GP, as shown in figure 2(b).

2.4 Plasma pinch during the post-fuelling

By comparing the line-integrated density from different channels, strong inward pinch effect can be observed during the post-SMBI phase. For the edge-most channels (Z = -17.5 and 24.5 cm), the line-integrated density begins to decrease several milliseconds right after the sharp increasing phase; however, the innermost channels (Z=±3.5cm) continuously increase for about 30 ms and then decrease, as shown in figure 3. Different post-SMBI behaviours between edge and core density channels indicate that inward particle pinch exists and its velocity is around 6 m/s estimated by the phase delay.

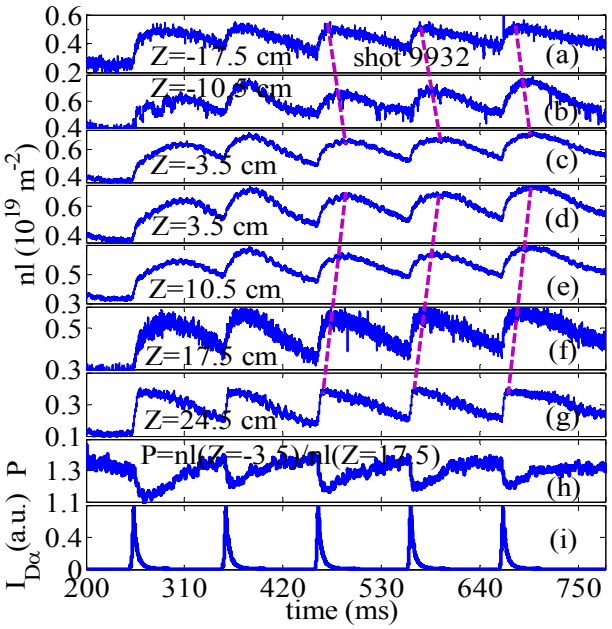

Figure 3. Phase delay of the line-integrated plasma density for different channels. (a)~(g) are line-integrated electron density; (h) peaking factor defined by the ratio of line-integrated electron density from Z=-3.5 and 24.5; (i) D_α monitoring the fuelling.

Furthermore, the time evolution of increment of plasma density (density difference between post-fuel and pre-fuel) indicates that the pinch exists during the post-fuel phase. As the increasing of density affected by neutral source is relatively less important because that the D_α is not so high during the slow density increasing phase, therefore, the time evolution of the density increment represents mainly the plasma transport features during the slow increasing phase. Compared with the density before GP pulse, the position of the maximum density increment are around r=30, 28 and 26 cm at 500, 510 and 520 ms, respectively, indicating that the increase of the line-averaged density is due to the

pinch effect, as shown in figure 4(a); In the case of SMBI, the position of maximum increment of density drifts inward as well; However, the density evolution measured by MWR is not well consistent with the line-averaged one by HCN because that the density of higher (lower) than 1.8 (0.8) $\times 10^{19}$m^{-3} measured by MWR is interpolated, as shown in figures 4(b) and 4(c). And the velocity of the pinch is around 2~3 m/s for GP and SMBI, estimated by the inward drift of the peak of increased density.

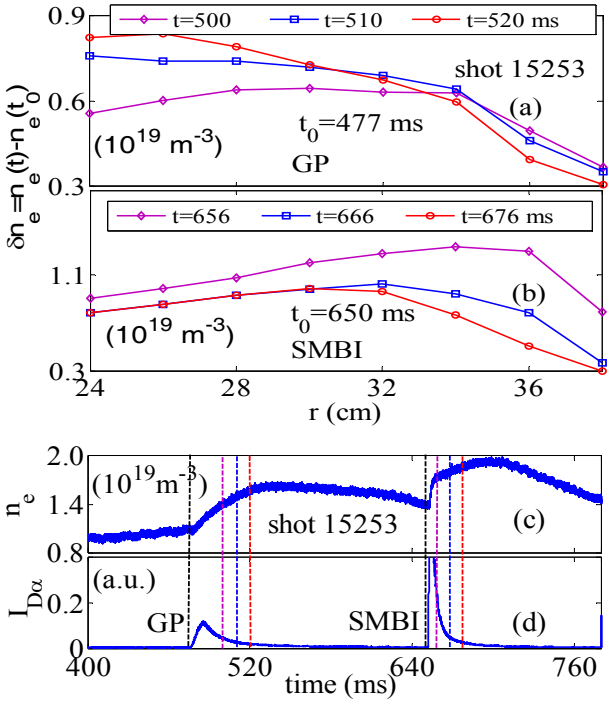

Figure 4. Comparison of the increment of electron density during the slow increasing phase. (a) and (b) the evolution of density increment for GP and SMBI by MWR, respectively; (c) line-averaged plasma density by HCN and (d) D_α monitoring the fuelling.

Comparison of post-fuelling normalized electron temperature gradient between SMBI and GP is conducted. For both SMBI and GP cases, $\delta T_e/T_e$ is increased, which indicates that the value of V/D is changed after the fuelling; in other words, the confinement is improved. However, there is some difference of $\delta T_e/T_e$ between SMBI and GP. The enhancement of $\delta T_e/T_e$ by SMBI can be up to twice as much as that of GP, especially at the beginning of the SMBI pulse.

3. Summary

The total fuelling efficiency of SMBI is up to twice as high as that of GP; the reasons for the higher fuelling efficiency of SMBI are mainly due to two aspects. One is higher percentage of neutrals injected by SMBI can enter the plasma; and the other is stronger convection induced by the SMBI.

Acknowledgments

This work is supported in part by the Chinese National Fusion Project for ITER under Grant No. 2010GB101001, and partially supported by the Nature Science Foundation of China under Grant No. 11005034.

References

[1] D. L. Yu *et al* 2010 *Nucl. Fusion* **50** 035009

[2] D. L. Yu *et al* 2012 *Nucl. Fusion* **52** 082001